SIMULATION OF STELLAR IMAGES FOR SCHMIDT PLATE ASTROMETRY

L. LANTERI[1], L. PIVIDORI[1], M.G. LATTANZI[2†] and B.M. LASKER[2]
[1] *Osservatorio Astronomico di Torino, Pino Torinese, Italy*
[2] *Space Telescope Science Institute — ST ScI, Baltimore, Maryland, U.S.A.*

1. Introduction

Schmidt plate-based surveys of the sky are currently the largest sources of positions and colours of stellar and non-stellar objects (see e.g. Lasker 1993). This situation is likely to remain such through the next decade when new and improved CCDs will probably replace the photographic medium. But even then deep photographic surveys will constitute important first epoch material for the derivation of better proper motions. Accordingly, we should do our best to improve astrometry and photometry of Schmidt plates.

We have developed a simulator for the production of realistic synthetic Schmidt plate star images. Such simulated images provide an ideal test-bed for applications such as the measurement of the performances of new photometric and astrometric algorithms. For example, the bright limit imposed by most of the astrometric reference catalogues available today makes it mandatory to customize new as well as traditional centring techniques to improve on the positions of saturated images. Our simulator can closely reproduce stellar profiles in density space over a wide range of magnitudes (from $V \simeq 6.5$ down to $V \simeq 19$), i.e. it can provide largely saturated images as well as those with an S/N close to the plate limit.

Although the numerical value of the relevant parameters have been optimized for the Guide Star Catalog surveys (1983 Quick-V in the North and 1975 ESO/SERC in the South — see Lasker et al. 1990), the simulation procedure should be applicable to most scanning machines and telescope/plate combinations.

2. The Simulator

The shape of the stars in intensity space are generated according to the circular symmetric model of Moffat (1969 and references therein); and it takes into account, besides seeing, diffraction and scattering within the emulsion. The model parameters are optimized via a trial and error procedure which compares the simulated profiles to a set of real stars with known photometry. For stars brighter than B = 16 on the deep southern plates, or brighter than V = 13 on the Quick-

† Affiliated with the Astrophysics Division, SSD, ESA; on leave from Torino Observatory.

V plates, two more important features become noticeable, namely the diffraction from the telescope spikes and the contribution from the filter. Other effects like corrector reflections and ghosts have not been included in this version of the simulator.

The filter intensity profile is a constant function of the distance from the halo centre, while the spike profile is generated using again a Moffat-like function which takes into account the cross-like shape of the spikes.

After several direct measurements of well exposed spikes and filter halos images, we have implemented the ratio 10^{-4}:2.5 x 10^{-3}:0.9949 for the energy contributions of filter, single spike, and star respectively. Transformation from *relative* intensity to density space is done through the plate characteristic curve, for which we use the representation in Lasker et al. (1990).

Noise processes include Poisson statistics, neighbouring pixel correlation, and PDS electronics. Poisson noise is intrinsic to the photons coming from stars and the sky background and is generated at the pixel level. By definition, the spatial correlation of Poisson noise is zero. However, the Quick-V or SERC/ESO plates have been scanned with an aperture roughly twice the size of the scanning step (which defines the pixel size). This generates fuzzier images and a patchier appearance of the sky regions, i.e. the scanning process has induced correlation among nearby pixels. Such correlation is simulated following the technique described in Lattanzi & Bucciarelli (1991), with the empirical correlation function derived from sky-only sections of the test plates. The typical correlation length is of $\simeq$ 1 pixel (radius). Finally, PDS noise is generated by the electronics of the microdensitometer. This noise source is noticeable when the density peaks above a certain limit and is maximum at the density cut-off when the current produced by the microdensitometer is lowest.
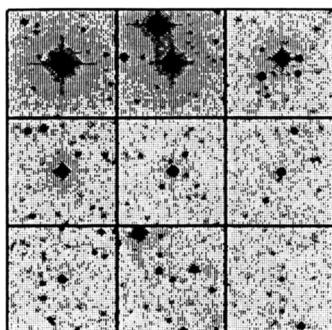

Figure 1 a)   Sequence of real stars of known magnitude from plate N081.   **Figure 1 b)** Simulation of the sequence in Fig. 1a.
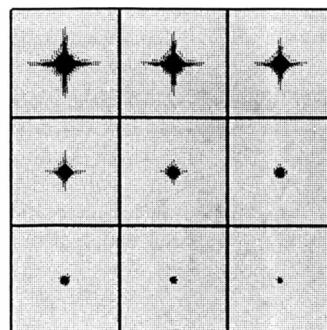
3. Results

Figure 1a shows a sequence of real stars (extracted from the digital copy of the Quick-V plate N081) whose magnitudes are known to better than 0.05^{mag}. The magnitude of the brightest star (centre of the top left panel) is $V = 6.67$ and that of the faintest (centre of the bottom right panel) is $V \simeq 15$, with increments of $\simeq 1^{mag}$ across the sequence. Figure 1b shows the same photometric sequence, generated by our simulator. Given the limitations of this version of the code, the resemblance is remarkable.

Acknowledgements

References

Lasker, B.M. et al. 1990. *Astron. J.*, **99**, 2019.
Lasker, B.M. 1993. In 'Databases for Galactic Structure', ed. A.G. Davis Philip, in press.
Lattanzi, M.G. and Bucciarelli, B., 1991. *Astron. Astrophys.*, **250**, 565.
Moffat, A.F.J., 1969. *Astron. Astrophys.*, **3**, 455.